Available online at www.sciencedirect.com

SciVerse ScienceDirect

Journal of the European Ceramic Society 32 (2012) 2451–2457

www.elsevier.com/locate/jeurceramsoc

Halogen plasma erosion resistance of rare earth oxide films deposited on plasma sprayed alumina coating by aerosol deposition

Jae-Hyun Jung [a,b], Byung-Dong Hahn [a], Woon-Ha Yoon [a], Dong-Soo Park [a,*], Jong-Jin Choi [a], Jungho Ryu [a], Jong-Woo Kim [a], Cheolwoo Ahn [a], Kie-Moon Song [b,**]

[a] *Functional Ceramics Research Group, Korea Institute of Materials Science, Changwon, Gyeongnam 641-010, South Korea*
[b] *Department of Applied Physics, Konkuk University, Chungju, Chungbuk 380-701, South Korea*

Received 7 September 2011; received in revised form 26 January 2012; accepted 12 February 2012
Available online 11 March 2012

Abstract

Dense yttria, erbia and dysprosia films with thicknesses of 44.8 ± 1.7, 51.6 ± 0.9 and 36.8 ± 3.1 μm, respectively, were deposited on plasma sprayed alumina coating by aerosol deposition (AD). The rare earth oxide films remarkably enhanced the erosion resistance of the plasma sprayed alumina coating upon exposure to the halogen gas plasma. The enhanced plasma erosion resistances were related to their low surface porosity as well as the low vapor pressures of the rare earth fluorides and chlorides compared with those of corresponding aluminum halogenides. Electrical breakdown voltages of the samples with yttria, erbia and dysprosia films on the plasma sprayed alumina coating were 5.5, 6.2 and 5.3 kV, respectively, at room temperature and 4.0, 4.2 and 3.9 kV, respectively, at 573 K. The breakdown voltages at RT and 573 K were more than double that of the plasma sprayed alumina coating without the AD films.

Keywords: Films; Surfaces; Corrosion; Y_2O_3

1. Introduction

Many ceramic parts are being used for semiconductor and flat-panel-display (FPD) processing equipments including electrostatic chuck (ESC), heater, gas distribution plate and others.[1] Some of those parts such as ESC require a high erosion resistance to corrosive gas plasma and breakdown voltage among others. As sizes of the parts were increased, manufacturing them by sintering becomes difficult and time-consuming. One alternative way to sintering large ceramic parts for semiconductor or FPD processing equipments is plasma spray coating on metal substrates.[2] Plasma spraying allows deposition of coatings up to a few centimeters in thickness.[3] However, plasma sprayed ceramic coatings often contained pores as big as 5–10 μm in size.[3] Pores in plasma sprayed ceramic coatings not only impaired the electrical properties but also experienced a severe attack by the halogen gas plasma as reported by Maeda and Shima[4] and Kim et al.[5] Recently, Kitamura et al. improved the microstructure and the properties of plasma sprayed yttria coating by axial suspension plasma spraying.[6]

Alumina has been one of the most widely used ceramics for the parts of semiconductor and FPD processing equipments. It has satisfied the requirements for electrical properties and erosion resistance to the corrosive gas plasma of the parts for the above equipments. However, recent progress in semiconductor and FPD processing employs higher density corrosive gas plasma than ever and alumina needs to be replaced with materials more resistant to the plasma erosion. The plasma erosion occurs in two ways; physical etching and chemical etching. Physical etching is also called as sputter etching and material removal occurs by highly accelerated ionic species striking the material's surface and breaking inter-atomic bonding on the surface. So, material with strong inter-atomic bonding would be desirable for the plasma erosion resistance. Chemical etching involves interaction between ionized species of the plasma and the material's surface to form volatile products. In that case, the plasma reaction product having low vapor pressure on the material's surface would improve the plasma erosion resistance. Kiyohara et al. reported that the plasma erosion resistance of hot-isostatically pressed yttria was more than three times that

* Corresponding author. Tel.: +82 55 280 3345; fax: +82 55 280 3392.
** Corresponding author. Tel.: +82 44 840 3628; fax: +82 44 851 4169.
E-mail addresses: pds1590@kims.re.kr (D.-S. Park), kmsong@kku.edu (K.-M. Song).

0955-2219/$ – see front matter © 2012 Elsevier Ltd. All rights reserved.
doi:10.1016/j.jeurceramsoc.2012.02.019

of hot-isostatically pressed alumina.[7] Although yttria exhibited excellent resistance to the plasma erosion, it required a high temperature above 1873 K to be sintered to a high density as reported by Kodo et al.[8] Not only difficulty in achieving a high density but also poor mechanical strength and high cost of sintered yttria limited its use for the parts of semiconductor processing equipments.

Aerosol deposition (AD) was reported to deposit highly dense ceramic films consisting of nano-scale crystallites.[7,9–11] Iwasawa et al. reported that density of yttria film deposited by AD exceeded 95% theoretical density (TD) and its erosion resistance against the $CF_4 + O_2$ plasma was about 40 times that of quartz.[10] According to Kiyohara et al., yttria film deposited by AD exhibited better resistance to the plasma erosion than sintered yttria due to the absence of surface pores where severe erosion occurred.[7] Although yttria film deposited by AD exhibited excellent resistance to the plasma erosion as described above, the residual stress in the film might limit its thickness to a few tens of micrometers.[11] Ceramic films with thickness of a few hundred micrometers are generally needed to survive the high voltage applied to some members of semiconductor or FPD processing equipments like ESC.[4] In this study, dense rare earth oxide films including yttria (Y_2O_3), erbia (Er_2O_3) and dysprosia (Dy_2O_3) films were deposited by AD on 222 μm thick plasma sprayed alumina coating in order to improve its halogen plasma erosion resistance and the electrical breakdown voltage.

2. Experimental procedure

2.1. Preparation of rare earth oxide films by aerosol deposition

Plasma sprayed alumina coatings on aluminum alloy disks with dimensions of 25 mm (diameter) × 5 mm (thickness) were prepared by Acecoat, Haman, Korea. The alumina coating was ground to have thickness of 222.5 ± 6.5 μm. The ground alumina surface with the average surface roughness (R_a) of 0.36 ± 0.03 μm was blasted with 200 grit alumina abrasive (99.6%, A&C Chemicals Pty. Ltd., Naranda, Australia) using 0.5 MPa compressed air to make R_a 1.79 ± 0.11 μm. The blasted alumina coatings were used as substrates for AD of the rare earth oxide films.

Commercially available yttria, erbia and disprosia powders were purchased from Uranus Chemicals Co., Ltd., Hsinchu, Taiwan. Yttria powder was heat treated at 1473 K for 2 h in air according to our previous experience. The powders were sieved using 100 mesh screen for breaking large soft agglomerates. Average particle sizes (d_{50}) of yttria, erbia and dysprosia powders after sieving were measured by a dry particle size analyzer (Helos & Rodos Windox 5, Sympatec GmbH, Clausthal-Zellerfeld, Germany) to be 3.55, 5.59 and 2.15 μm, respectively. The sieved powders were used for AD. Details of AD procedure were described in the previous report.[11] The substrate surface was 10 mm off the nozzle and reciprocally moved at 10 mm/s for 15 times. Compressed air from a medical grade air compressor carried fine particles of the rare earth oxide and sprayed them onto the substrate through a nozzle with 35 mm × 0.8 mm slit type opening. Flow rate of the compressed air was 10 L/min. The powder feed rate was approximately 0.6 kg/h. During AD, pressure in the deposition chamber was about 920 Pa. Plasma sprayed alumina coating sample, yttria film, erbia film, and dysprosia film were named as sample A, Y, E and D, respectively.

2.2. Characterization

Surfaces of the four samples were analyzed using X-ray diffractometer (D-Max 2200, Rigaku Co., Tokyo, Japan). They were cleaned in an ultrasonic bath and sputter-coated with gold for SEM (JSM-5800, Jeol Co., Tokyo, Japan) observation. Density was measured by liquid immersion method using Xylene. Surfaces of the samples were polished down to 1 μm diamond paste. Some samples were cut, mounted using epoxy and polished down to 1 μm diamond paste for examining the cross section. Ten different locations on the cross section SEM micrograph of each sample were selected for measuring thickness of the AD film. Cross sections of some samples were examined using HR-TEM (JEM-2100F, Jeol, Tokyo, Japan). TEM samples were prepared using FIB (Vion, FEI, Hilsboro, Oregon, USA). Breakdown voltage was measured both at room temperature and at 573 K according to ASTM D149-97 using a fixture with two titanium electrodes of 30 mm in diameter.[12] High voltage was applied between the two electrodes in silicone oil for avoiding discharge. A withstanding voltage tester (TOS 5101, Kikusui Electronics Corp., Yokohama, Japan) was used for breakdown voltage of the sample. The voltage was applied at a rate of 500 V/s. Three disks were tested for each sample.

Plasma erosion tests were carried out using a dry etching machine (BEP-5000, ICP-etching System, SN Tek, Gimpo, Korea) at National Center for Nanomaterials Technology, Pohang, Korea. Based on the information obtained from semiconductor industry, two kinds of plasma erosion tests were performed; erosion by plasma of CF_4 + Ar gas mixture and erosion by plasma of $Cl_2 + BCl_3$ gas mixture. Gas flow rates were 45 sccm for CF_4 and Cl_2 and 15 sccm for Ar and BCl_3. Chamber pressure was 1.3 Pa, Source power and bias power were 800 W and 500 W, respectively. For each plasma erosion test, the four samples were placed on ESC and eroded together for 0.5 h. Surface of each sample was partially covered with small piece of silicon wafer during erosion. After plasma erosion, the height difference between eroded and un-eroded surface of each sample was measured with a surface profilometer (Perthometer PGK 120, Mahr GmbH, Göttingen, Germany) for obtaining erosion depth. Erosion rate was obtained by dividing the erosion depth by the exposure time (0.5 h). X-ray photoelectron spectroscopy (XPS, Escalab 250 XPS spectrometer, VG Scientific Ltd., UK) was performed on the surfaces eroded by the plasma.

3. Results

Fig. 1 shows XRD patterns of samples A, Y, E and D. Only alumina peaks (both α and γ phase) were detected from samples

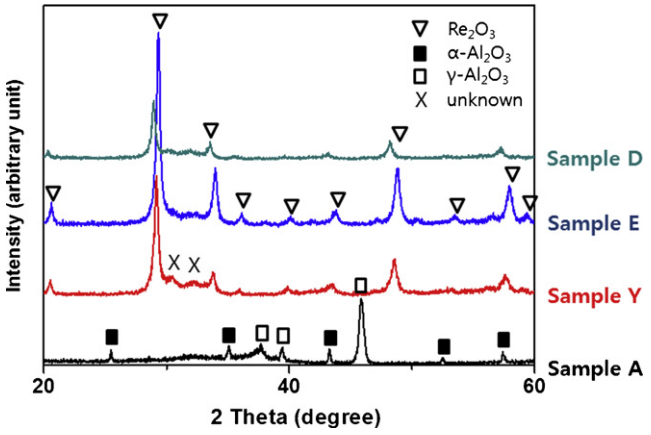

Fig. 1. XRD patterns from samples A, Y, E, and D.

A while yttria, erbia and dysprosia peaks as well as two small unknown peaks were detected from samples Y, E and D, respectively. The three rare earth oxides have cubic structures with different lattice parameters that shifted the patterns slightly as shown in Fig. 1. Although XRD patterns of the rare earth oxide powders are not shown here, intensity of the peaks from samples Y, E and D was much weaker than that of the corresponding powders. Full widths half maximum (FWHM) of the rare earth oxide powders measured at about 29.23° 2θ were 0.209°, 0.254° and 0.155° for Y_2O_3, Er_2O_3 and Dy_2O_3 powders, respectively. On the other hand, those of the corresponding AD films were 0.344°, 0.366° and 0.347° for samples Y, E and D, respectively. While plasma sprayed alumina coating contained a significant amount of pores, few pore was observed from the rare earth oxide films as shown in Fig. 2(a)–(c). Density of the rare earth oxide film was 96.1%, 94.9% and 94.3% TD for samples Y, E and D, respectively. TD of Y_2O_3, Er_2O_3 and Dy_2O_3 were 5.03, 8.64 and 7.81 g/cm^3, respectively, as obtained from the literature.[13] The polished surfaces of samples Y, E and D were very smooth; R_a values of those surfaces were 0.055 ± 0.008, 0.026 ± 0.004 and 0.015 ± 0.002 μm, respectively, while those of the samples before polishing were 1.689 ± 0.122, 1.570 ± 0.099 and 1.670 ± 0.180 μm, respectively. Interface of the rare earth oxide film and plasma sprayed alumina coating was microscopically wavy and surface pores of the alumina were filled with the rare earth oxide film. Thicknesses of yttria, erbia and dysprosia films of the polished samples Y, E and D were 44.8 ± 1.7, 51.6 ± 0.9 and 36.8 ± 3.1 μm, respectively. Fig. 3(a) and (b) shows the alumina coating and the alumina/dysprosia film interface of sample D, respectively. While alumina grain away from the interface and dysprosia grain showed relatively good crystallinity as shown in Fig. 3(a) and (b), alumina near the interface had many small regions with poor crystallinity as indicated by the circles in Fig. 3(b). Fig. 4 shows the breakdown voltages at room temperature and 573 K; the error bar represents the minimum and the maximum measured values of each sample. Average breakdown voltages of the samples A, Y, E and D at room temperature were 2.7, 5.5, 6.2 and 5.3 kV, respectively. At 573 K, average breakdown voltages of samples A, Y, E and D were reduced to 1.6, 4.0, 4.2 and 3.9 kV, respectively.

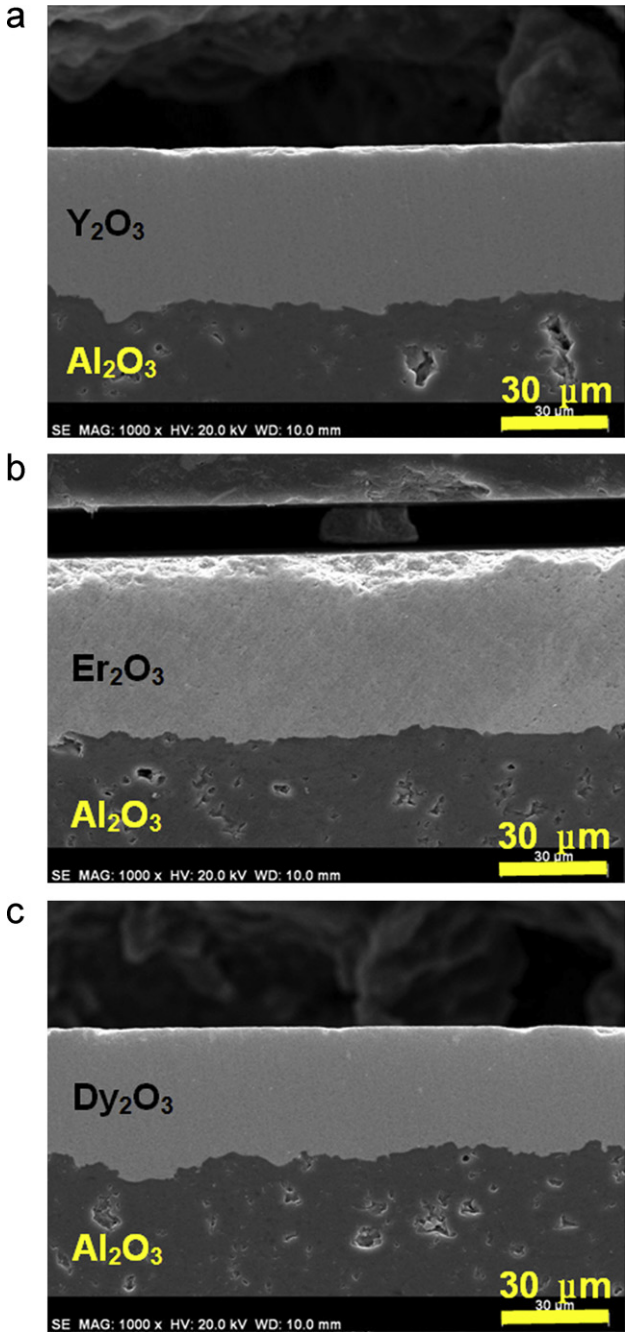

Fig. 2. SEM micrographs of cross sections of the samples: (a) sample Y, (b) sample E, and (c) sample D.

Fig. 5 shows erosion rates of the samples exposed to CF_4 + Ar plasma. Sample A was eroded at 11.3 μm/h. On the other hand, the erosion rates of the other three samples were 1.3, 1.4 and 1.0 μm/h for samples Y, E and D, respectively. Fig. 6(a)–(d) shows surfaces of the samples before and after exposure to the plasma. Sample A was severely attacked by the plasma. Not only pores originally present on the surface appearing in Fig. 6(a) but also entire surface was attacked by the plasma as shown in Fig. 6(b). Fig. 6(c) shows the polished surface of sample D where very fine surface pores appearing as dark spots were scattered over the entire surface. After the plasma erosion, the surface

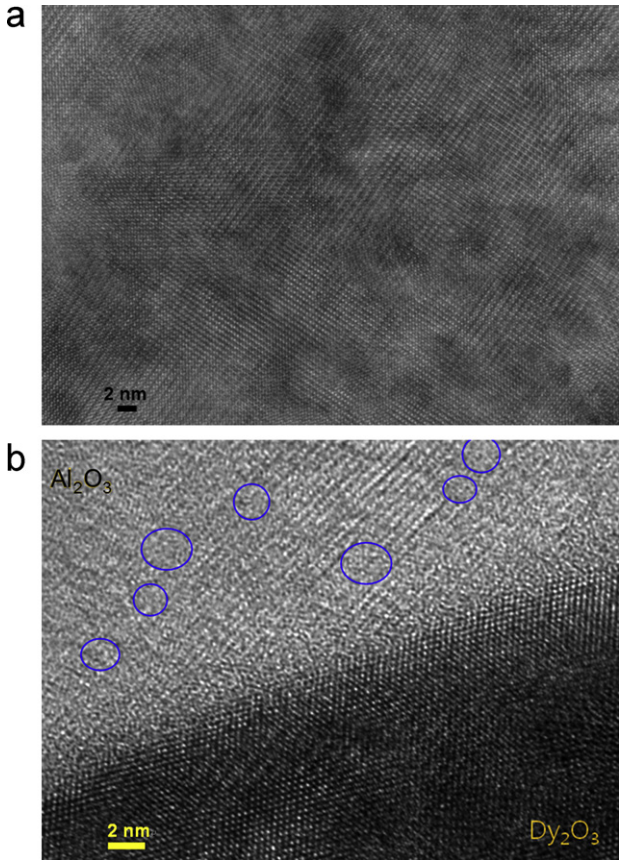

Fig. 3. HR-TEM micrograph of sample D: (a) alumina grain away from the interface between the alumina and dysprosia film and (b) interface between the alumina and dysprosia film showing dysprosia grain with a good crystallinity directly contacted with alumina containing fine localized regions of poor crystallinity as indicated by the circles.

became slightly rough as shown in Fig. 6(d). Fig. 7 shows erosion rates of the samples after exposure to $Cl_2 + BCl_3$ plasma. The erosion rates were lower than those exposed to $CF_4 + Ar$ plasma; 1.8 μm/h for sample A, 0.3 μm/h for sample Y, 0.4 μm/h for sample E and 0.3 μm/h for sample D. Fig. 8(a)–(d) shows

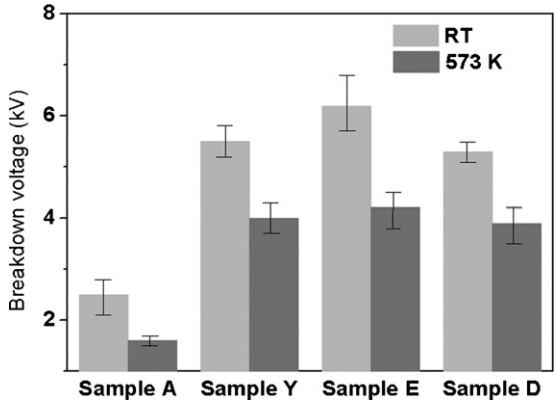

Fig. 4. Breakdown voltages of the samples measured at room temperature and 573 K; at room temperature, sample A ranging from 2.1 to 2.8 kV, sample Y from 5.2 to 5.8 kV, sample E from 5.7 to 6.6 kV, sample D from 5.1 to 5.5 kV; at 573 K, sample A from 1.5 to 1.7 kV, sample Y from 3.7 to 4.3 kV, sample E from 3.8 to 4.5 kV, sample D from 3.5 to 4.2 kV.

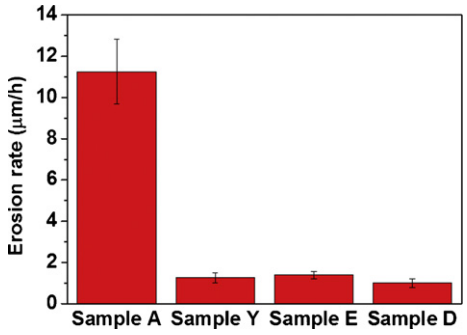

Fig. 5. Erosion rates of the samples exposed to $CF_4 + Ar$ plasma.

surfaces of the samples after exposure to $Cl_2 + BCl_3$ plasma. In case of sample A, the attack by the plasma was concentrated on pores and alumina grains were delineated on the smooth area as shown in Fig. 8(a). Fine surface pores of the rare earth oxide films grew by the plasma attack as shown in Fig. 8(b)–(d). All the samples show less surface damage when exposed to the $Cl_2 + BCl_3$ plasma than when exposed to the $CF_4 + Ar$ plasma. Fig. 9(a) shows XPS spectra from the surfaces after $CF_4 + Ar$ plasma erosion. Strong peaks of rare earth element–fluorine bond were observed from samples Y, E and D while intensity of Al–F bond peak from sample A was much weaker. Fig. 9(b) shows XPS spectra of the surfaces after $Cl_2 + BCl_3$ plasma erosion. Rare earth element–chlorine bond peaks were detected from samples Y, E and D but they were much weaker than rare earth element–fluorine bond peaks in Fig. 9(a). Al–Cl bond peak was hardly detected from sample A. Surface profiles on eroded and un-eroded areas of samples A and Y are shown in Fig. 10.

4. Discussion

AD has been considered as a novel method for making dense ceramic films.[9] In order to deposit dense thick films on a substrate by AD, it is important to have a strong interface between the film and the substrate. The strong interface is accomplished through so-called "anchor layer" that is formed by fine particles stuck into the substrate upon impingement during AD as described in the literature.[9,10] However, when the substrate is as hard as alumina, it would be difficult to stick the rare earth oxide particle into the substrate to make the "anchor layer". One strategy for mimicking the "anchor layer" is making the substrate surface microscopically rough by grit blasting. The roughened surface would increase the contact area between the film and the substrate. As a matter of fact, yttria film thicker than 20 μm is detached from the as-ground smooth surface of plasma sprayed alumina coating used for this study due to lack of strong adhesion. Grit blasting in this study makes the alumina surface microscopically rough enough for deposition of the rare earth oxide films with over 30 μm in thickness without peeling off as shown in Fig. 2(a)–(c). Fig. 2(a)–(c) also clearly demonstrate that pores on the alumina surface are sealed with the rare earth oxide films. Alumina grains away from the interface with the AD rare earth oxide film exhibit good crystallinity as shown in Fig. 3(a) while the small regions indicated by the circles in Fig. 3(b) in the alumina near the interface exhibit poor

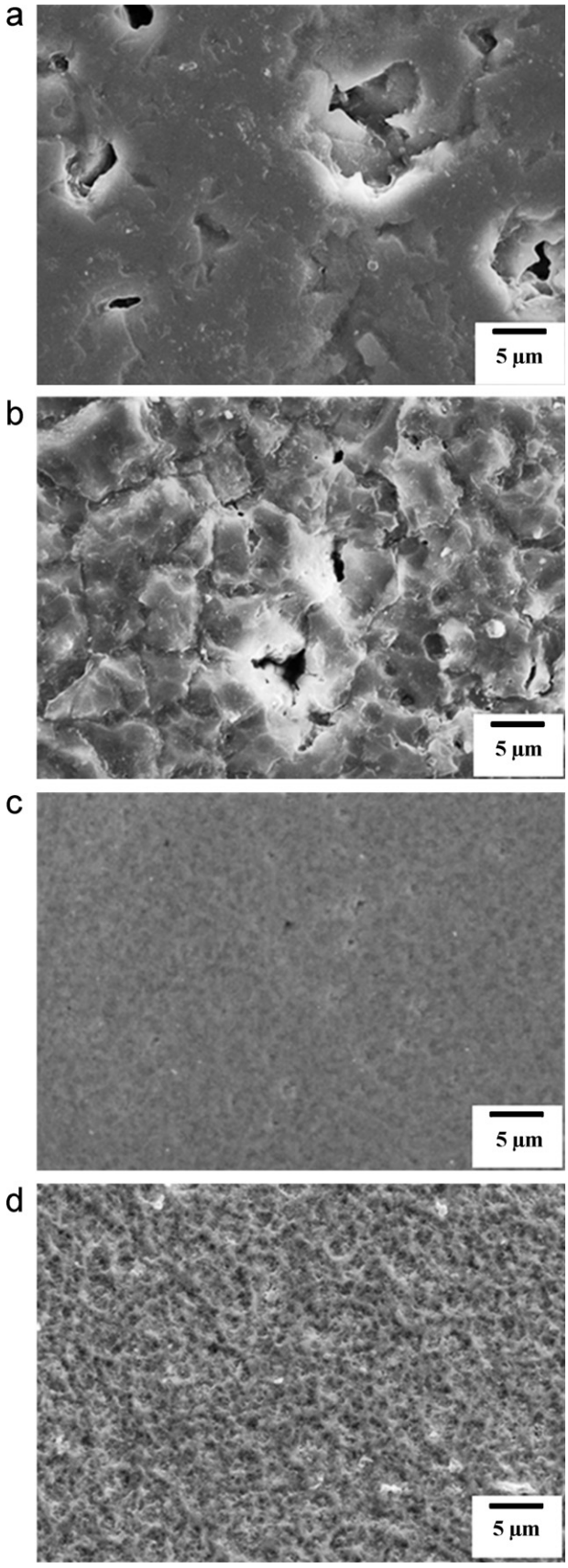

Fig. 6. SEM micrographs of the sample surfaces before and after exposure to $CF_4 + Ar$ plasma for 0.5 h: (a) and (b) sample A, (c) and (d) sample D; (a), (c) before exposure and (b), (d) after exposure.

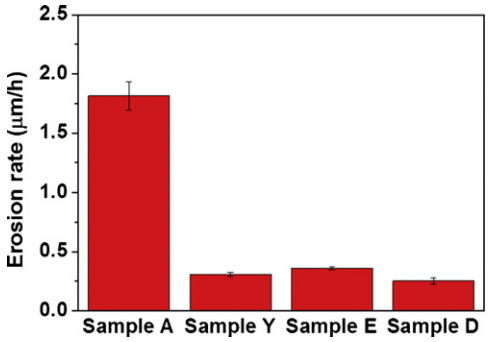

Fig. 7. Erosion rates of the samples exposed to $Cl_2 + BCl_3$ plasma.

crystallinity. Both grit blasting and AD drive the ceramic particles fast to collide with the plasma sprayed alumina surface. Since the size and impact energy of the alumina grits during the grit blasting are larger than those of the rare earth oxide particles during AD, the plasma sprayed alumina is possibly damaged during grit blasting and those small regions with poor crystallinity may be formed. It is also noted that the AD rare earth oxide film is in direct contact with the alumina as shown in Fig. 3(b). Breakdown field strength is strongly influenced by porosity of the dielectrics as reported on plasma sprayed alumina coatings by Kitamura et al.[2] Highly dense ceramic films deposited by AD exhibit an excellent breakdown field strength as reported by Kiyohara et al.[7] Although breakdown field strength that is breakdown voltage divided by thickness of the dielectric material is used for characterizing the dielectrics, breakdown voltage itself also counts in some practical applications like ESC.[4] We take advantage of both plasma spraying for thick coating and AD for highly dense film. Fig. 4 demonstrates that breakdown voltage is more than doubled by depositing the dense rare oxide films on the plasma sprayed alumina coating in spite of the fact that thickness of the rare earth oxide film is less than one quarter that of the alumina coating. According to Kitamura et al., electrical breakdown field strength of the plasma sprayed yttria coating is similar to that of the plasma sprayed alumina coating.[2] Therefore, the remarkable improvement in breakdown voltage shown in Fig. 4 is considered to result from high density of the rare earth oxide films that effectively seal off the surface of plasma sprayed alumina coating. Difference in breakdown voltages among samples Y, E and D is qualitatively consistent with thickness difference of the three rare earth oxide films.

$CF_4 + Ar$ gas plasma is used for etching oxides while $Cl_2 + BCl_3$ gas plasma for etching Al metal in semiconductor industries. Except Ar, all the gases above are chemically reactive and participated in chemical erosion to produce fluorides and chlorides. When the reaction product is not volatile, it might interfere with further removal of the material. Vapor pressure of AlF_3 is higher than the rare earth fluorides as shown in Table 1. High vapor pressure of AlF_3 explains in part why the erosion rate of sample A is the higher than those of the other samples with the rare earth oxide films as shown in Fig. 5. Although vapor pressures of the other fluorides are low as shown in Table 1, they are in the order consistent with the erosion rates of the samples shown in Fig. 5. Strong rare earth element–fluorine bond peaks

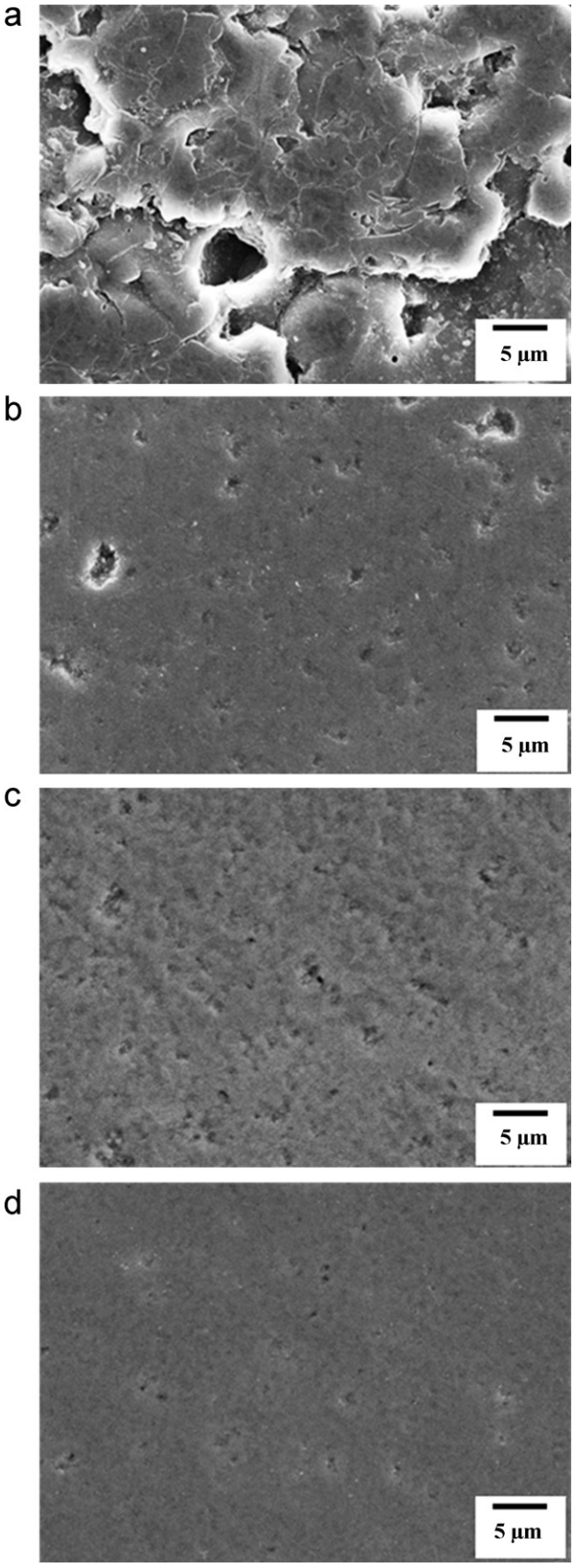

Fig. 8. SEM micrographs of the sample surfaces after exposure to $Cl_2 + BCl_3$ plasma for 0.5 h: (a) Sample A, (b) sample Y, (c) sample E, and (d) sample D.

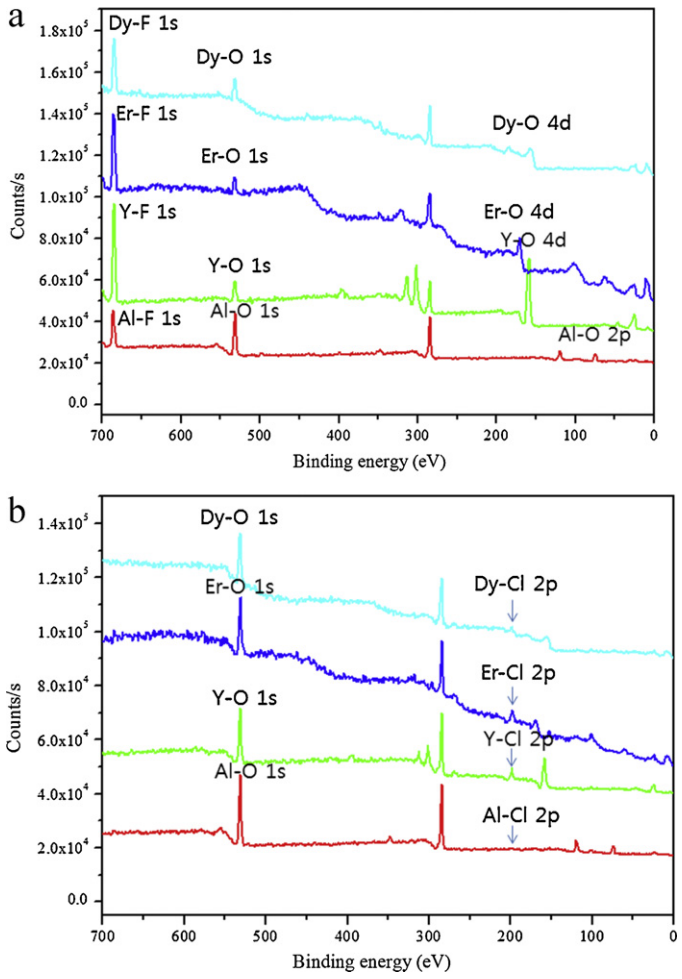

Fig. 9. XPS spectra from the sample surfaces eroded by (a) $CF_4 + Ar$ plasma and (b) $Cl_2 + BCl_3$ plasma.

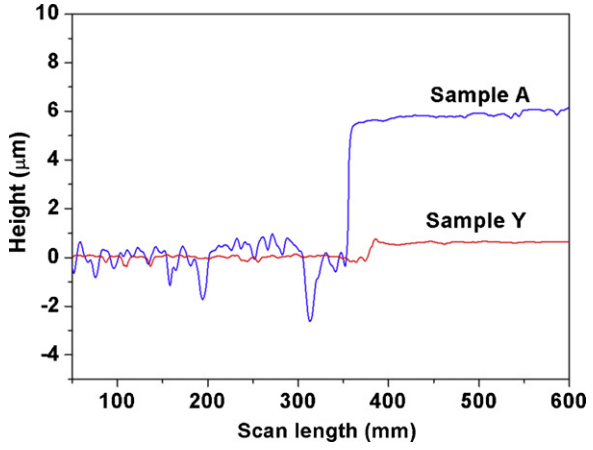

Fig. 10. Surface profiles of samples A and Y after the $CF_4 + Ar$ plasma erosion test.

from samples Y, E and D shown in Fig. 9(a) suggest the presence of bigger amount of the rare earth fluorides on the surfaces during $CF_4 + Ar$ plasma erosion than aluminum fluoride on sample A. Ar ion beam attacks the samples by breaking atomic bonding. Bond strengths of Al–O, Y–O, Er–O and Dy–O are reported as 511, 719, 615 and 607 kJ/mol, respectively.[13] The weakest

Table 1
Vapor pressures of the fluorides and chlorides.

Compound	Vapor pressure (Pa)	Compound	Vapor pressure (Pa)
AlF_3	4@973 K[15]	$AlCl_3$	1795@400 K[16]
YF_3	0.28@1434 K[17]	YCl_3	8.11@973 K[19]
ErF_3	0.49@1437 K[18]	$ErCl_3$	8.64@1043 K[19]
DyF_3	0.24@1437 K[18]	$DyCl_3$	7.18@1023 K[19]

Al–O bond explains in part why alumina is severely attacked by CF_4 + Ar Plasma. Vapor pressure of $AlCl_3$ is higher than those of the rare earth chlorides as shown in Table 1, and they are related to the XPS spectra shown in Fig. 9(b). Weak rare earth element–chlorine bond peak from samples Y, E and D suggests the presence of the corresponding rare earth chlorides on the surface that might interfere with further attack by the plasma. On the other hand, XPS spectra from surface of the eroded sample A suggest the absence of the chloride on the surface that allows further attack by the plasma. Both Table 1 and Fig. 9(b) are consistent with the erosion rates of the samples shown in Fig. 7. The higher erosion rates by CF_4 + Ar plasma than those by $Cl_2 + BCl_3$ plasma might be explained in part by stronger reactivity of the former than the latter.

Ceramic films deposited by AD often exhibit network looking surface morphology due to fine height difference between hills and valleys as previously reported.[14] Trace of the network looking morphology still remains after polishing as shown in Fig. 6(c) although R_a was as small as 0.015 μm. Erosion occurs over the entire surface but the valley is attacked more than the hills by the gas plasma, making the network looking surface morphology clear as shown in Fig. 6(d). As shown in Fig. 10, the step height between the two areas of sample Y is remarkably smaller than that of sample A supporting the difference in erosion rates. Another thing worth mentioning is the roughness difference between the two areas of sample A. It is clearly recognized that the surface pores grow deep as well as wide and the smooth surface is also damaged during the erosion. In other words, the pores are subjected to intensive erosion as reported in the literature.[4,5] In case of sample Y, the surface undulation is exaggerated by the erosion even though it is not so much as in sample A. Smooth surface with smallest undulation should be beneficial to the plasma erosion resistance.

5. Conclusion

Dense yttria, erbia and dysprosia films with thicknesses between 36.8 μm and 51.2 μm were deposited on the plasma sprayed alumina coating by aerosol deposition. The grit blasting of the alumina coating produced a suitable surface roughness for making the thick rare earth oxide films by AD. Microscopically wavy interface between the alumina coating and the rare earth oxide film allowed deposition of those films without peeling off. The rare earth oxides sealed off surface pores of the plasma sprayed alumina coating and doubled the breakdown voltage. The three rare earth oxide films exhibited about 5 times stronger resistance to the plasma erosion than the plasma sprayed alumina coating. Their excellent plasma erosion resistance can be explained in part by the low vapor pressures of the rare earth fluorides and chlorides.

Acknowledgment

This work has been supported in part by Inter-Institutional Cooperation Research Program of ISTK.

References

1. Matsuhiro K, Sakaguchi S. Trends of research and development on engineering ceramics. *Ceram Jpn* 2006;**41**:195–8.
2. Kitamura J, Ibe H, Yuasa F, Mizuno H. Plasma sprayed coatings of high-purity ceramics for semiconductor and flat-panel-display production equipment. *J Therm Spray Technol* 2008;**17**:878–86.
3. Gansert LRV. Plasma sprayed ceramic coatings. *Ceram Ind* 2001;**152**:48–52.
4. Maeda T, Shima S. High dielectric strength member. US Pat Appl No. 10/737,785; 2003.
5. Kim D-M, Kim K-B, Yoon S-Y, Oh Y-S, Kim H-T, Lee S-M. Effects of artificial pores and purity on the erosion behaviors of polycrystalline Al_2O_3 ceramics under fluorine plasma. *J Ceram Soc Jpn* 2009;**117**:863–7.
6. Kitamura J, Tang Z, Muzuno H, Sato K, Burgess A. Structural, mechanical and erosion properties of yttrium oxide coatings by axial suspension plasma spraying for electronics applications. *J Therm Spray Technol* 2011;**20**:170–85.
7. Kiyohara M, Hatano H, Iwasawa J. A new plsama resistant coating reducing particle generations. *J Vac Soc Jpn* 2010;**53**:573–7.
8. Kodo M, Soga K, Yoshida H, Yamamoto T. Low temperature sintering of polycrystalline yttria by transition metal ion doping. *J Ceram Soc Jpn* 2009;**117**:765–8.
9. Akedo J. Aerosol deposition of ceramic thick films at room temperature: densification mechanism of ceramic layers. *J Am Ceram Soc* 2006;**89**:1834–9.
10. Iwasawa J, Nishimizu R, Tokita M, Kiyohara M, Uematsu K. Plasma-resistant dense yttrium oxide film prepared by aerosol deposition process. *J Am Ceram Soc* 2007;**90**:2327–32.
11. Hahn B-D, Kim K-H, Park D-S, Choi J-J, Ryu J, Yoon W-H, et al. Fabrication of lead zirconate titanate thick films using a powder containing organic residue. *Jpn J Appl Phys* 2008;**47**:5545–52.
12. *ASTM D149-97a: standard test method for dielectric breakdown voltage and dielectric strength of solid electrical insulating materials at commercial power frequencies*. ASTM International; 2009.
13. Lide DR. *CRC handbook of chemistry and physics*. 81st ed. Boca Raton: CRC Press; 2000.
14. Hahn B-D, Park D-S, Choi J-J, Ryu J, Yoon W-H, Kim K-H, et al. Dense nanostructured hydroxyapatite coating on titanium by aerosol deposition. *J Am Ceram Soc* 2009;**92**:683–7.
15. Jacoboni C, Perrot O, Boulard B. Vapour-phase deposition of rare-earth-doped PZG glasses. *J Non-Cryst Solids* 1995;**184**:184–9.
16. Vlola JT, Seegmiller DW, Fannin Jr AA, King LA. Vapor pressure of aluminum chloride systems. 1. Vapor pressure and triple point of pure aluminum chloride. *J Chem Eng Data* 1977;**22**:367–70.
17. Batsanova LR. Rare-earth fluorides. *Russ Chem Rev* 1971;**40**: 465–73.
18. Besenbruch G, Charlu TV, Zmbov KF, Margrave JL. Mass spectrometric at high temperatures. XVII. Sublimation and vapor pressures of Dy(III), Ho(III) and Er(III) fluorides. *J Less-Common Met* 1967;**12**:375–81.
19. Moriarty JL. Vapor pressure of yttrium and rare earth chlorides above their melting points. *J Chem Eng Data* 1963;**8**:422–4.